*Journal of Power Sources*, 30 (1990) 257 - 267


# DETERMINATION OF DISCHARGE TIME AND CAPACITY BY SHORT-PERIOD DISCHARGE METHOD

ALEKSANDAR B. DJORDJEVIC

*Gandyeva 61/IX, 11070 Belgrade (Yugoslavia)*

## Introduction

The voltage ($U_p$)/time ($t$) discharge curves of batteries have been rarely used to characterize the behaviour of such systems. In particular, there is scope to examine the initial stages of the typical 'S' shape of the discharge curve, *i.e.*, when $t \ll 1$. Such a study is possible when the circuit is closed rapidly [1, 2] and data acquisition is obtained precisely. The beginning of the discharge curve should reflect the entire discharge curve.

The aim of this work is to predict the discharge time, capacity, energy and power of a given battery for given discharge conditions (load, temperature, etc.) using data obtained from a short-duration discharge. This method would cause negligible decrease in the capacity of the battery.

## Experimental

The analysis was conducted on experimental data obtained previously. The cells were discharged continuously through constant loads at room temperature, to a final voltage $U_{pd} = U_o/2$. A mercury relay was used to close the circuit in a time between 0.1 and 0.3 s.

An HP 3054 DL Computer and a Y–t plotter were used to determine and record discharge voltage as a function of time. The results lacked precision because of the small resolution and long start time. This caused difficulties in the analyses. Alkaline manganese cells (LR 20-VARTA) were used to demonstrate the new method for determining battery characteristics.

The mathematical calculations were conducted on an IBM personal computer using Symphony software.

## Theoretical background

The method for predicting the discharge time is based on the definition of the discharge curve in 3D-space. This is described by the coordinates:

$$\log t\text{—}R\text{—}U_p \tag{1}$$

0378-7753/90/$3.50 

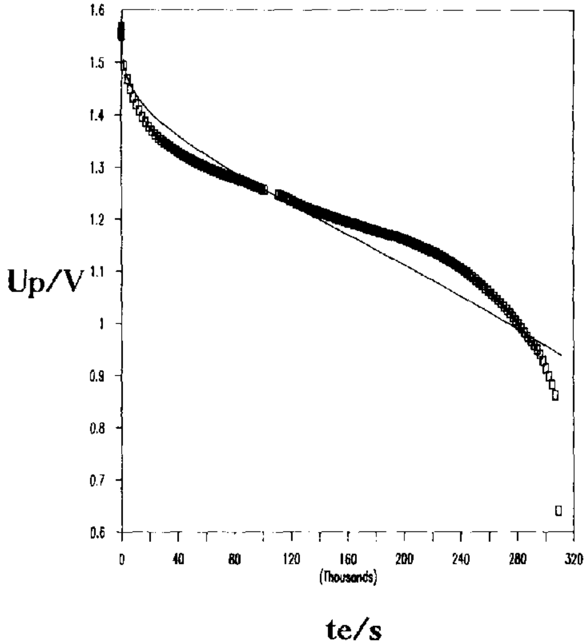


Fig. 1. Discharge curves (experimental, e, and calculated, r, eqns. (2) and (5)) for alkaline manganese cell (LR 20-VARTA, $R_p = 10\ \Omega$); (□) Experimental $U_{pe}$; (——) calculated, $U_{pr}$, from eqns. (2) and (5).

where:

$$R = U_p/(U_l - U_p) \tag{2}$$

and $U_l$ is a linearizing voltage.

Equation (2) is derived from the relationship [4] for the internal resistance of the battery (or cell), *i.e.*,

$$R_i = R_p(U_o - U_p)/U_p \tag{3}$$

when the open-circuit voltage, $U_o$, is replaced by the linearising voltage, $U_l$. Electrochemical measurement (the difference $(U_l - U_o)$ may be used to determine the internal resistance) of the replacement can be achieved by analysing the initial part of the curve, probably from $10^{-6}$ s.

Figure 1 shows a complete discharge curve for an alkaline managanese LR 20-VARTA cell discharged through a $10\ \Omega$ load. This discharge lasts for 85.6 h and gives a capacity of 10.22 A h. The open-circuit voltage, $U_o$, is 1.5905 V.

Figure 2 shows the same curve as a logarithmic function of $t_e$. Projections of the areas along the coordinate $P$ are on the coordinate plane. The $U_p$ *versus* log $t$ curves for $U_l = U_o$ and $U_l = U_r$ differ along the time coordinate. Figure 3 illustrates that $U_{pe}$ and $U_{per}$ give the same area ($C_e$ and $C_r$) with the time coordinate. The projections of the areas that are independent of the time

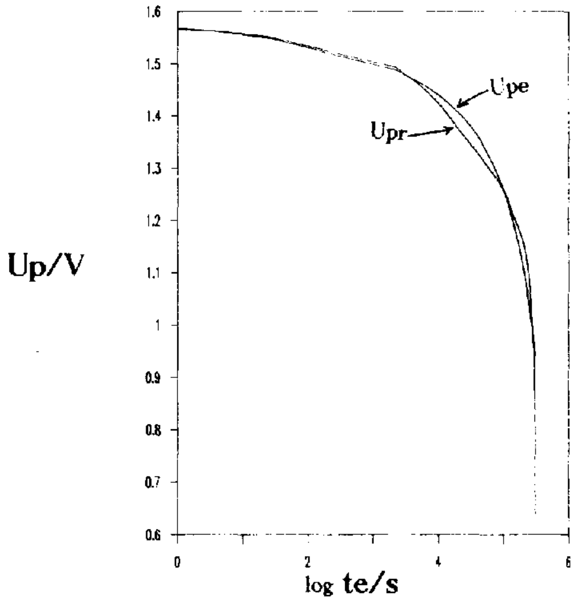


Fig. 2. Discharge curves (experimental, e and calculated, r, eqns. (2) and (5)) for alkaline manganese cell; (LR 20-VARTA, $R_p = 10\,\Omega$). $U_{pe}$ experimental; $U_{pr}$ calculated from eqns. (2) and (5).

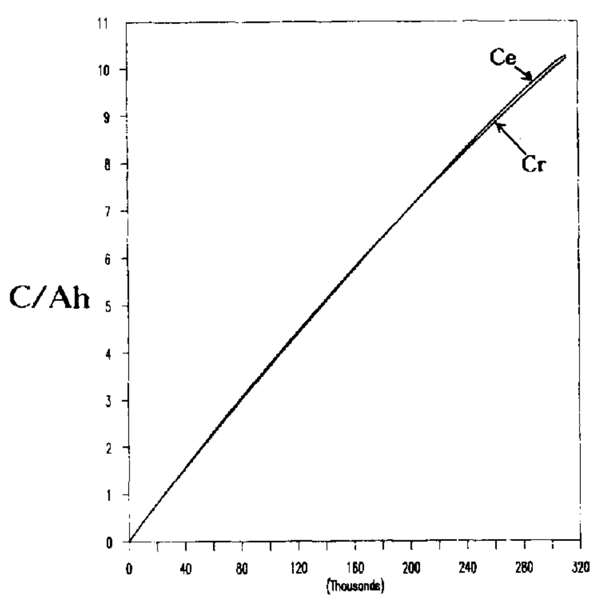


Fig. 3. Capacity of (experimental, e and calculated, r, eqns. (2) and (5)) alkaline manganese cell (LR 20-VARTA, $R_p = 10\,\Omega$. $C_e$ experimental; $C_r$ calculated using eqns. (2) and (5).

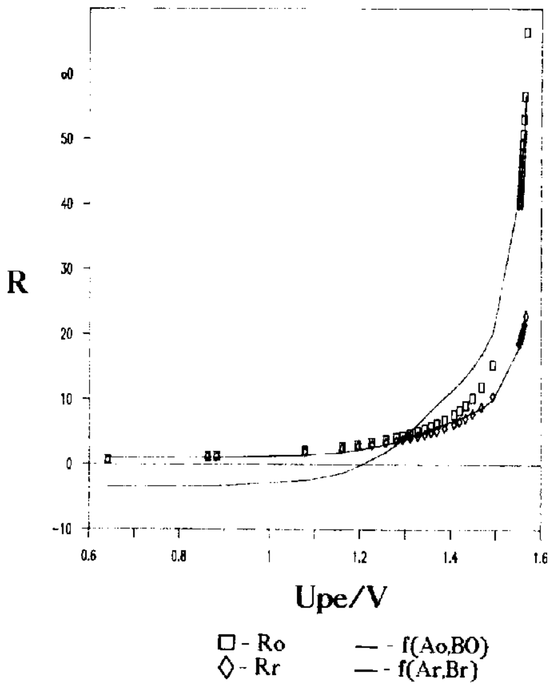


Fig. 4. Resistance relations-$R$ (eqns. (2) and (5), $U_1 = U_o$ and $U_1 = U_r$) *vs.* experimental discharge voltage for alkaline manganese cell (LR 20-VARTA $R_p = 10\,\Omega$).

coordinate are on the coordinate plane of the $U_{pe}$ *versus* $R$ plot (Fig. 4). By changing the value from $U_1 = U_o$ to $U_1 = U_r$ ($U_1 <> U_o$, $U_1 = U_r$ when $R^{2\max}$), the areas $U_p$—$R$ change position in space. At the intersections of the pairs of areas are the discharge curves in 3D-space:

- $U_{peo} = f(U_1, U_{pe}, t_e)$, $U_1 = U_o$
- $U_{pso} = f(U_1, A_o, B_o, t_e)$, $U_1 = U_o$

. . . . . . . . . . . . . . . . . . . . . . . . . . . . . . . . . . . . . . . . . . . . . . . .

- $U_{pel} = f(U_1, U_{pe}, t_e)$, $U_o <> U_l <> U_r$
- $U_{psl} = f(U_1, A_l, B_l, t_e)$, $U_o <> U_l <> U_r$

. . . . . . . . . . . . . . . . . . . . . . . . . . . . . . . . . . . . . . . . . . . . . . . .

- $U_{pr} = f(U_1, U_{pe}, t_e)$, $U_1 = U_r$
- $U_{psr} = f(U_1, A_r, B_r, t_e)$, $U_1 = U_r$

The curves (Fig. 5): $R_o$—l—r $= f(U_1, U_{pe}, t_e)$ are obtained by linearization of the projection of the discharge curve in 3D-space ($U_{peo}$—l—r/V) on the plane: log $t_e$—R. The straight lines: $R_o$—l—r $= f(A_o$—l—r, $B_o$—l—r, $t_e)$ from these projections are obtained by regression analysis:

$$R_o = A_o = B_o \log t_e \quad (U_1 = U_o, R^2 < R^{2\max}) \tag{4}$$

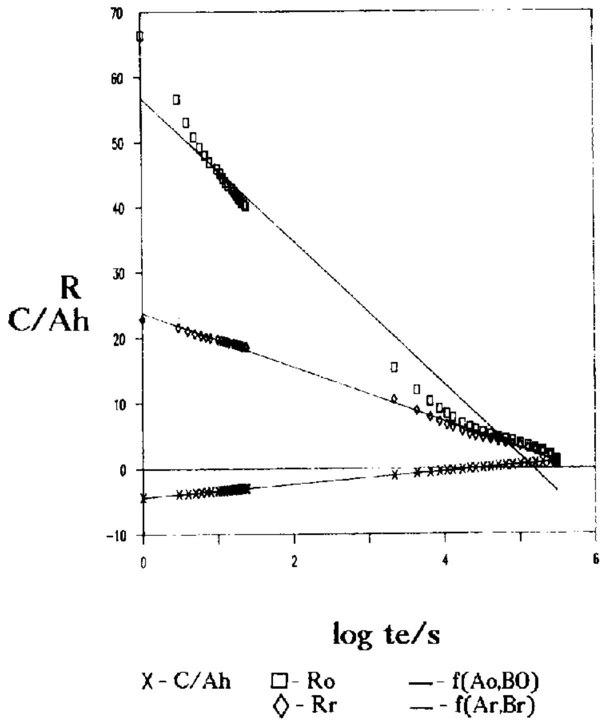


Fig. 5. Resistance relations-$R$ [eqns. (2) and (4), $U_l = U_o$ and $U_l = U_r$] *vs.* time for alkaline manganese cell (LR 20-VARTA, $R_p = 10\,\Omega$).

up to straight line:

$$R_r = A_r + B_r \log t_e \quad (U_l = U_r,\ R^{2\,\max}) \tag{5}$$

From these straight lines and by introducing $R_r$ into eqn. (2), the $U_{pso}$—l—r curves can be calculated.

The analogue of the time method (coordinate $\log t$) is the capacity method (coordinate $\log C$) in 3D-space: $\log C$—$R$—$U_p$. Figure 6 shows the changes in the regression coefficients of $R_l = f(U_l, U_{pe}, t_e)$ and $R_l = f(U_l, U_{pe}, C_e)$ over the change interval between $U_l = U_o$ and $U_l > U_r$.

The equations for predicting the discharge time (and capacity) are derived from eqn. (2). Tangents to the discharge curve according to:

$$U_p t = U_p^2/U_l + [(U_l - U_p)^2/U_l]R \tag{6}$$

define the end of the discharge at $R = 1$:

$$\log t_d = \log t_n + (U_l - 2U_{pn})/((U_l - U_{pn})B) \tag{7}$$

where: $n = 1 \ldots k$ and $k$ is the number of experimental points, $U_{pn}$ is $U_{pen}$ or $U_{psn}$.

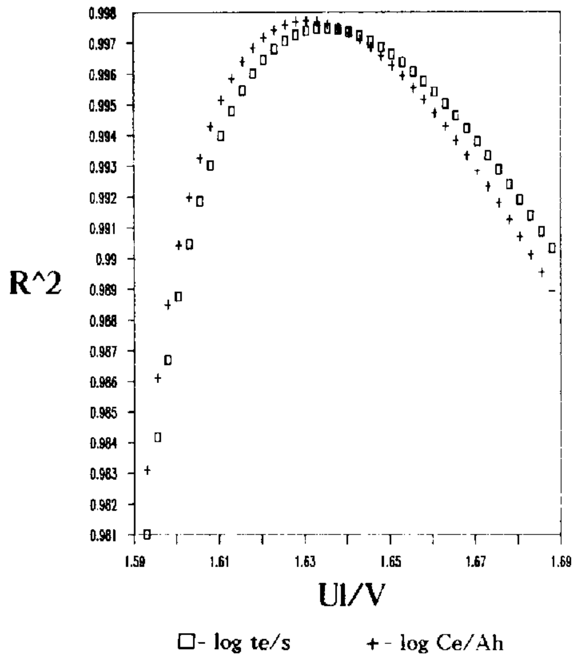


Fig. 6. Regression coefficients-$R^2$ ($R = f(\log t_e)$ and $R = f(\log C_e)$) *vs.* linearising voltage $U_l$ for alkaline manganese cell (LR 20-VARTA, $R_p = 10\,\Omega$).

Secants, the analogues to the tangents:

$$U_{ps} = U_{p1} \times U_{p2}/U_l + [(U_l - U_{p1})(U_l - U_{p2}/U_l]R \tag{8}$$

define the end of the discharge at $e = 1$ for small distances between the points on the curve and precise determination:

$$\log t_d = \log t_m + \frac{(\log t_n - \log t_m)(U_l - 2U_{pm})(U_l - U_{pn})}{U_l(U_{pn} - U_{pm})} \tag{9}$$

where: $m = n - 1$; $n = 1 \ldots k$ and $k$ is the number of experimental points, $U_{pm}$ is $U_{pem}$ and $U_{pn}$ is $U_{pen}$. When $U_{pm}$ and $U_{pn}$ are $U_{psn}$ and $U_{psm}$, respectively, the results from eqns. (7) and (9) are identical.

The tangents and secants penetrate the smooth surface: $R = R_p/R_i = 1$ (parallel to the coordinate plane: $U_p$ — $\log t$) at the discharge times, when $U_l = U_r$. Figure 7 shows these penetration points along the time coordinate:

- $t_pS_o$ secants $U_{pe}$ for $U_l = U_o$, eqn. (9)
- $t_pT_o$ tangents $U_{pe}$ for $U_l = U_o$, eqn. (7)
- $t_pT_{so}$ tangents $U_{ps}$ for $U_l = U_o$, eqn. (7)
- $t_pS_r$ secants $U_{pe}$ for $U_l = U_r$, eqn. (9)
- $t_pT_r$ tangents $U_{pe}$ for $U_l = U_r$, eqn. (7)
- $t_pT_{sr}$ tangents $U_{ps}$ for $U_l = U_r$, eqn. (7)

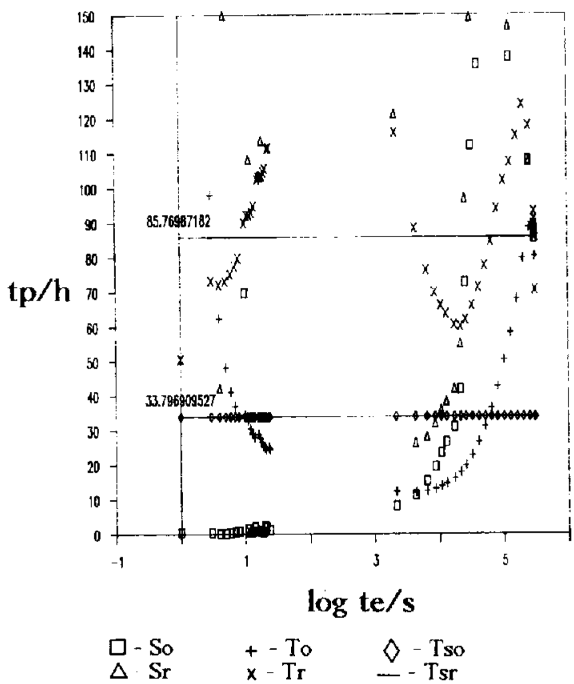


Fig. 7. Calculated discharge times $t_p$ ($R = 1$, secants-S and tangents-T, $U_l = U_o$ and $U_l = U_r$) *vs.* time for alkaline manganese cell (LR 20-VARTA, $R_p = 10\ \Omega$).

The penetration points of the tangents ($U_{pn}$ is $U_{pen}$, eqn. (7) and secants ($U_{pm,n}$ are $U_{pem,n}$, eqn. (9)) on the discharge curve in 3D-space depend on the time coordinate. The linearized discharge curves in 3D-space are at curved surfaces. The predicted discharge time is the mean value of all penetration points.

The penetration points of both the tangents ($U_{pn}$ is $U_{psn}$, eqn. (7)), and the secants ($U_{pm,n}$ are $U_{psm,n}$, eqn. (9)) on the discharge curves that are derived from the straight lines are independent of the time coordinate (85.77 h, Fig. 7). The discharge curves in 3D-space from the straight lines are at plane surfaces.

Curved and plane surfaces are parallel to the coordinate: $U_p$. Points of the penetration of the secants are dispersed and this means poor accuracy. For precise time and capacity predictions, linearization and regression require equal intercepts on the time or capacity coordinate (Figs. 4 - 7, 40 points and Figs. 8 - 11, 20 points, for regression analyses) and measurement of the first point at the earliest stage possible.

To generate predicted $U_p$ and $C$ values, shorter intercepts (Figs. 1 - 3, 160 points) are recommended on the time or capacity coordinates.

## Results

It has been shown that linearization of the total discharge curve of a battery reproduces the characteristics of the power source. Application of this method to predict the discharge time and capacity requires the initial part of the discharge curve ($U_{p1} \ldots U_{pk}$, $k \ll n$) to be linearized, not the total curve ($U_{p1} \ldots U_{pn}$). The initial part must be as short as possible, must take a negligible amount of the capacity, and must not provoke self-discharge in the battery.

Figure 8 shows the change in the regression coefficients for an alkaline manganese cell (LR 20-VARTA) discharged through a 10 Ω load. Data acquisition was achieved on an HP 3054 DL unit and, therefore, fast acquisition up to 24 s (1 s intervals) is not precise. Slow acquisition is at 360 s steps, and greater. Therefore, the interval: $24\ \mathrm{s} < t_e < 10^5\ \mathrm{s}$ is used, see Fig. 9. The predicted discharge time is 93.789 h, *i.e.*, the capacity is 10.01 A h. Figures 10 and 11 show the change in the regression coefficients and predicted discharge time for the alkaline manganese cell (LR 20-VARTA) through a 2.5 Ω load, $U_o = 1.5930$ V. The experimentally measured discharge time is 17.54 h and the capacity 8.38 A h. Data acquisition has been carried out using fast plotters for a period of 30 s ($5\ \mathrm{s\ cm^{-1}}$, $20 \times 10^{-3}\ \mathrm{V\ cm^{-1}}$). Twenty points have been read

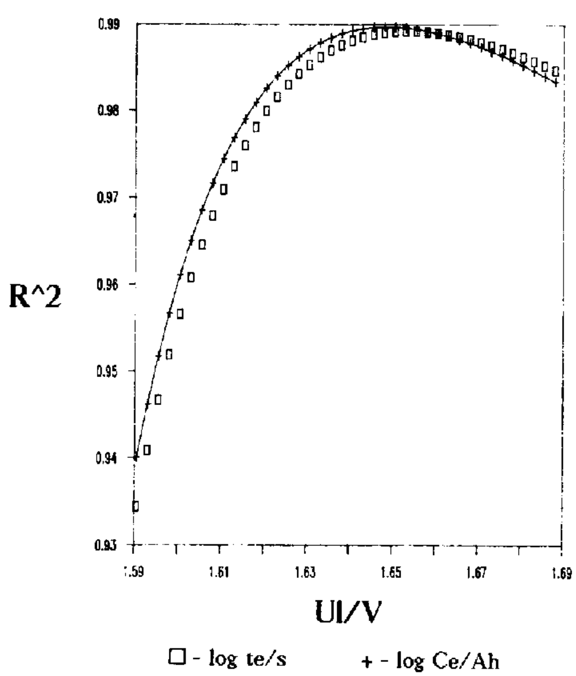


Fig. 8. Regression coefficients $R^2$ ($R = f(\log t_e)$ and $R = f(\log C_e)$) *vs.* linearising voltage-$U_l$ for alkaline manganese cell (LR 20-VARTA, $R_p = 10\ \Omega$).

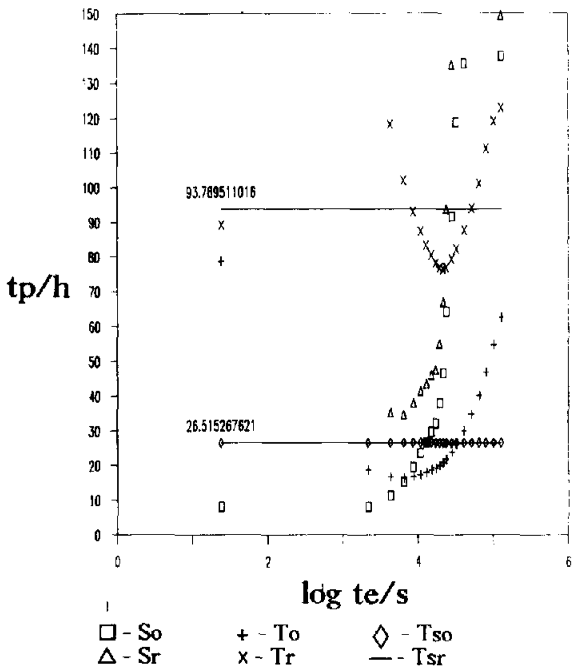


Fig. 9. Calculated discharge times $t_p$ ($R = 1$, secants-S and tangents-T, $U_l = U_o$ and $U_l = U_r$) *vs.* time for alkaline manganese cell (LR 20-VARTA, $R_p = 10\ \Omega$).

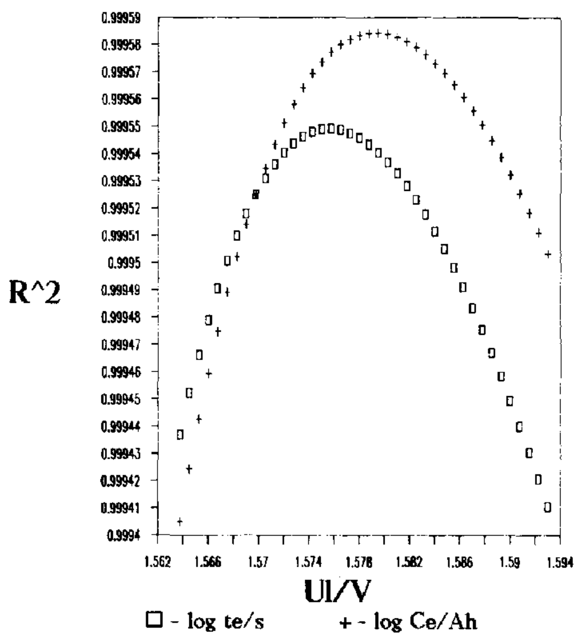


Fig. 10. Regression coefficients $R^2$ ($R = f(\log t_e)$ and $R = f(\log C_e)$) *vs.* linearizing voltage $U_l$ for alkaline manganese cell (LR 20-VARTA, $R_p = 2.5\ \Omega$).

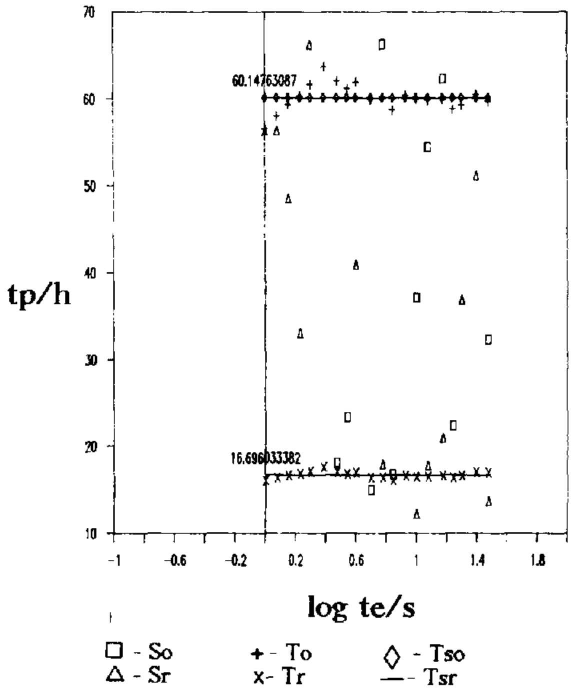


Fig. 11. Calculated discharge times $t_p$ ($R$ = 1, secants-S and tangents-T, $U_1 = U_o$ and $U_1 = U_r$) *vs.* time for alkaline manganese cell (LR 20-VARTA, $R_p$ = 2.5 Ω).

from the graph at relatively equal intervals of log $t_e$. The predicted discharge time is 16.696 h (Fig. 11) and the predicted capacity is 9.22 A h.

Similar results have been obtained with:

(i) alkaline managanese cells LR 20-VARTA discharged through 3.3 and 5 Ω loads;

(ii) pocket electrode, vented nickel/cadmium cells (AK-1 KRUSIK) discharged through a 1 Ω load;

(iii) sintered cylindrical electrode, sealed, nickel/cadmium cells (VR-4, SAFT) discharged through 2.5 Ω.

## Conclusions

The method of linearization of the initial part of the discharge curve of a cell or battery along the time or capacity coordinate allows predictions to be made of the discharge time and capacity. The reliability of the method depends on the time required to close the discharge circuit and the speed and precision of the time/voltage data acquisition. Further evolution and verification of the method will be achieved by collecting appropriate experimental data. This work will be directed towards:

(i) determining whether the method is applicable to all types of cells;

(ii) analysing other criteria, besides $R^{2\max}$, for determination of the end point;

(iii) examining the initial part of the discharge curve as a function of the internal resistance of a given cell and the components of this resistance.

**Acknowledgements**

The author thanks Mr V. Nakic and other associates of IHTM-Beograd and CVVSRM-Split for helpful discussion and assistance with the experiments.

**List of symbols**

| | | | |
|---|---|---|---|
| $U_o$ | Open-circuit voltage (V) | $C$ | Capacity (A h) |
| $U_p$ | Discharge voltage (V) | $A$ | Segment |
| $U_l$ | Linearizing voltage (V) | $B$ | Slope |
| $R_p$ | Discharge load (Ω) | $R^2$ | Regression coefficient |
| $R_i$ | Internal resistance (Ω) | $t$ | Time (s or h) |
| $R$ | Resistance relation | | |
| $T$ | Temperature (°C) | | |

*Indices*

| | | | |
|---|---|---|---|
| o | $U_l = U_o$ | e | Experimental |
| r | $U_l = U_r$, $R^{2\max}$ | l | Linearized |
| d | End of discharge | s | $f(A, B)$ |

**References**

1 S. Okazaki, S. Higuchi, N. Kubota and S. Takahashi, *J. Appl. Electrochem.*, *16* (1986) 513.
2 S. Okazaki, S. Higuchi, N. Kubota and S. Takahashi, *J. Appl. Electrochem.*, *16* (1986) 631.
3 A. B. Djordjevic, V. Nakic, N. Radic and A. Mihajlovic, *Tenth Yugoslav. Electrochemistry Symp., Becici, Yugoslavia, 1987.*
4 B. V. Beljajev, *Rabotosposobnost kimiceskih istocnikov toka*, Svjaz., Moskva, 1979.